Appl. Magn. Reson. 23, 557–569 (2003)

Applied Magnetic Resonance

Structural Analysis of Three-Spin Systems of Photosystem II by PELDOR

A. Kawamori[1], N. Katsuta[1], and H. Hara[2]

[1] School of Science and Technology, Kwansei Gakuin University, Sanda, Japan
[2] Bruker Biospin K.K., Tsukuba, Japan

Received September 14, 2002; revised October 23, 2002

Abstract. The pulsed electron electron double resonance (PELDOR) pulse sequence is applied to a three-spin system consisting of three radicals ($Y_D^{\bullet}$, $Y_Z^{\bullet}$ and Q_A^{-}) generated in spinach PS II. The distance between Y_Z and Q_A has been determined to be 3.4 nm with the previously derived distances of the other radical pairs, 2.9 nm for $Y_D^{\bullet}$-$Y_Z^{\bullet}$ and 3.9 nm for $Y_D^{\bullet}$-Q_A^{-}. This distance has been derived from the $Y_Z^{\bullet}$-Q_A^{-} radical pair trapped in Y_D-less mutants of *Chlamydomonas reinhardtii*. Furthermore the method was applied to the $Y_D^{\bullet}$-Q_A^{-}-Chl_Z^{+} system to find the unknown distance between Q_A and Chl_Z. The derived distance was 3.4 nm. A triangular configuration was found in the membrane system that gives the relative positions of the electron transfer components.

1 Introduction

In higher plants, photosystem II (PS II) is composed of several intrinsic and extrinsic membrane protein complexes. Among them, the heterodimer consisting of D1 and D2 proteins is believed to bind almost all the electron transfer components of PS II [1]. In Fig. 1 a supposed model structure on the basis of a bacterial reaction center is shown [2]. On the donor side, the primary electron donor P680 (a chlorophyll dimer), the secondary donor Y_Z (tyrosine-161 in the D1 subunit) and a cluster of four manganese atoms in the water-oxidizing complex (WOC) are contained. On the acceptor side, one of two pheophytin molecules accepts an electron from oxidized P680 and donates it to the primary electron acceptor plastquinone (Q_A). Besides, there are several additional redox-active components, namely, cytochrome *b*-559, chlorophyll Z (Chl_Z) (a monomer chlorophyll donor) and one more redox-active tyrosine residue Y_D (tyrosine-161 in the D2 subunit) in PS II [1].

Upon illumination the first charge separation occurs between P680 and pheophytin within a few hundred picoseconds and the electron on pheophytin is transferred to the first acceptor quinone within a few microseconds. Then the electrons transfer to the second acceptor quinone Q_B in the dark. The secondary donor

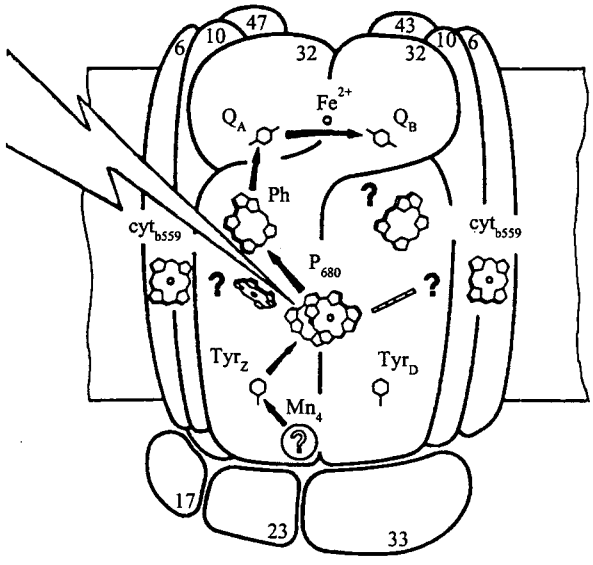

Fig. 1. Supposed model structure of PS II taken from ref. 2 with a modification. Arrows show electron transfers induced by light absorption.

tyrosine Z (Y_Z) provides an electron to P680 within the sub-microsecond range. The oxidized $P680^+$ has a short lifetime at physiological temperatures and was observable only by time-resolved absorbance spectroscopy [3]. The oxidized $Y_Z^{\bullet}$ has also a short lifetime, because WOC provides rapidly an electron. The manganese cluster accumulates oxidized equivalents by absorption of light quanta and evolves one oxygen molecule returning to the original reduced state after absorption of four light quanta. This process was found by Kok et al. [4] and is called Kok's oxygen clock or S-state cycle. The role of Y_D, Chl_Z and cytochrome *b*-559 has not yet been clarified in detail, and they have functioned as auxiliary electron donors in one of the side electron transfer paths. $Y_D^{\bullet}$ is a stable radical in the dark which has been studied in detail.

For a long time, crystallization of PS II was found to be difficult compared to other photosytems, such as bacterial reaction centers and PS I, because of the instability of WOC. Recently the crystallization of PS II of cyanobacterial photosystem was successful and X-ray structural analysis has been applied with a resolution of 0.38 nm. Most of the chlorine type pigments, as well as iron and the manganese clusters were recognized [5].

Meanwhile, several EPR methods have been applied to elucidate the location of the electron carriers in PS II [6–11]. In previous works, the dipole interactions between the paramagnetic species in PS II were probed by the PELDOR (pulsed electron double resonance) [12]. The pulse scheme employed was the three-pulse electron spin echo (ESE) sequence, in which microwave (mw) pulses with two different frequencies were used. This method has been developed by

Milov et al. [13] in the early 1980s to study the distribution of spin-labeled polymers in solution, where the distance between the labels was statistically distributed and the exponentially decaying spin echo intensities were analyzed [13]. On the other hand, the PS contains an isolated radical pair consisting of a donor and an acceptor with a definite distance. Its PELDOR gives an oscillating time profile with a definite frequency. From the time profile with a frequency of 2.7 MHz the distances between the manganese-cluster in the S_2 state and tyrosine D (Y_D) was derived to be 2.74 nm [12].

The "2 + 1" ESE technique used in ref. 12 is a special case of the general PELDOR method. It employs a sequence of three mw pulses with the same carrier frequency and is applicable when the EPR transitions of the paramagnetic centers under investigation can be efficiently excited by the pulses. The distance between Y_D and Y_Z in PS II was for the first time directly estimated to be 2.96 ± 0.05 nm with the "2 + 1" ESE method [14]. The accuracy in the distance is 0.05 to 0.1 nm, which is much higher than that for the present X-ray analysis, though it measures the separation between the centers of distributed spin density. To elucidate the electron transfer mechanism in detail, an accurate distance determination by pulsed EPR methods is anticipated.

We have determined several distances in nonoriented PS II membranes and their orientations relative to the membrane normal in oriented membranes [15]. Most of the distances were given for Y_D, because its radical is always existing in PS II. Other radicals were usually trapped during the electron transfer or observed by a time-resolved method after laser excitation such as in spin-polarized radical electron spin echo envelope modulation (ESEEM) [16, 17]. However, the distance and its orientation did not give the configuration of the electron transfer components as a whole. In this work the PELDOR technique was applied to a system consisting of three radical species Q_A^-, $Y_D^\bullet$ and $Y_Z^\bullet$ and the distance between Q_A and Y_Z was determined in addition to distances of Q_A-Y_D and Y_D-Y_Z obtained so far by PELDOR of the two spin systems. In addition, PELDOR experiments of the radical systems of $Y_D^\bullet$-Q_A^--Chl_Z^+ were carried out to determine the unknown distance between Q_A and Chl_Z. Finally, a configuration of these radicals was shown graphically. With the results of triangular spin configurations and the data obtained so far for two-spin systems, we have derived the coordinates of the electron transfer components relative to Y_D at the origin.

2 Experimental

2.1 Materials

Oxygen-evolving PS II membranes were prepared from market spinach by the method of Kuwabara and Muratra [18]. Oriented membranes were prepared according to Rutherford [19] by brushing PS II particles on mylar sheets and drying them under 90% humidity. Five or six sheets were stacked and inserted in a quartz tube with an inner diameter of 4 mm. Tris treatment was performed by

incubating PS II membranes on ice for 30 min in 0.8 M Tris buffer at pH 8.5 under room light to eliminate Mn clusters and extrinsic proteins. After centrifugation, to eliminate magnetic couplings with nonheme iron on the acceptor side, the pellet was suspended in $ZnCl_2$ containing buffer to substitute the nonheme iron by Zn^{2+} [20]. The suspension was centrifuged again and the obtained pellet was transferred into quartz tubes with a final chlorophyll concentration of about 20 mg/ml. The Y_D-less mutant was prepared as described in ref. 21 to eliminate the magnetic coupling with the $Y_D^{\bullet}$ radical spin systems.

The radical systems with $Y_D^{\bullet}$-$Y_Z^{\bullet}$-Q_A^{-} were trapped by illuminating the Tris-treated Zn-substituted PS II sample for 20 s at 253 K. The sample was immediately put into liquid nitrogen. To prepare $Y_D^{\bullet}$-Q_A^{-}-Chl_Z^{+}, Tris-treated PS II membranes were illuminated at 200 K for 10 min and immediately trapped at 77 K.

2.2 PELDOR Measurements

PELDOR was observed with an ESP380 spectrometer (Bruker) with the pulse sequence shown in Fig. 2b. The spectrometer was equipped with a cylindrical di-

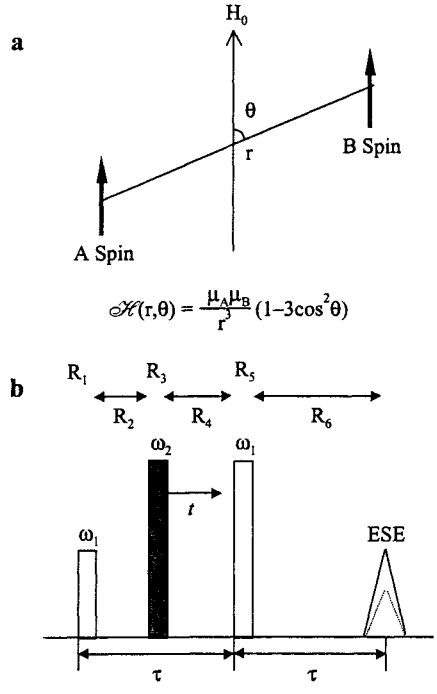

Fig. 2. Dipolar interaction between a radical pair (**a**) and pulse sequence for PELDOR (**b**). The first and the third pulse with frequency ω_1 form the spin echo of the A spins. The second pulse with frequency ω_2 rotates the B spins by 180°. The R_is denote operators in the rotating frame of spin A.

electric resonator (ER4117DHQ-H, Bruker) and a nitrogen gas-flow system (CF935, Oxford Instruments). A second microwave synthesizer HP83751 supplied mw power to a separate pulse former-unit. The measurement temperature was about 80 K and mw pulses of 80, 152, 152 ns duration were used. The pulse amplitudes for this sequence were adjusted to give spin rotation angles of 90°, 180° and 180°, respectively. These long-period pulses which excite only a narrow range of the broad radical signal were used to avoid spurious ESEEM signals.

3 Theory

In the beginning, we consider a spin system composed of pairwise-distributed radicals, with each pair consisting of spins A and B, $S^A = S^B = 1/2$. In the PELDOR experiment, three mw pulses were used to excite the spin system (Fig. 2b). The first and the third pulse, separated by the time interval τ, has a carrier frequency ω_1 resonant with the EPR transitions of the A spins and form the primary ESE signal of these spins. The second pulse, separated from the first pulse by the time interval t ($t \leq \tau$), has a carrier frequency ω_2. This pulse is resonant with the B spins and changes their projections from $|\alpha\rangle$ to $|\beta\rangle$, and vice versa. If the magnetic dipole interaction between the pairwise-distributed spins is appreciable, the flip of the B spin changes the local magnetic field of its partner in the pair (A spin). As a result, after the third pulse the magnetization of the A spins cannot be completely refocused at time 2τ and the amplitude of the primary ESE signal exhibits an oscillation which depends on the second-pulse position (i.e., on t).

The spin Hamiltonian for this system can be written as

$$\mathscr{H}/\hbar = \omega_A S_Z^A + \omega_B S_Z^B + D_{AB} S_Z^A S_Z^B,$$

in which ω_A and ω_B are the resonance frequencies of the isolated A and B spins, and D_{AB} represents the dipole coupling between the A and B spins, as given by

$$\hbar D_{AB} = g_A g_B \beta^2 (3\cos^2\theta - 1)/r_{AB}^3.$$

In the rotating frame with angular frequency ω_1, the spin Hamiltonian that affects the A spins is given by

$$\mathscr{H}/\hbar = (\Delta\omega_A + D_{AB} M_S^B) S_Z^A,$$

in which M_S^B is the quantum number associated with $S_Z^B = \pm 1/2$ and $\Delta\omega_A = \omega_A - \omega_1$ is the resonance offset of the A spins.

The density matrix at time 2τ is written as

$$\rho(2\tau) = R_6^\dagger R_5^\dagger R_4^\dagger R_3^\dagger R_2^\dagger R_1^\dagger S_Z^A R_1 R_2 R_3 R_4 R_5 R_6,$$

where the R_is are rotating operators given by

$$R_1 = \exp(i\pi S_X^A/2), \qquad R_2 = \exp(i\mathcal{H}t/\hbar),$$
$$R_3 = \exp(i\pi S_X^B), \qquad R_4 = \exp[i\mathcal{H}(\tau - t)/\hbar],$$
$$R_5 = \exp(i\pi S_X^A), \qquad R_6 = \exp(i\mathcal{H}t/\hbar).$$

After time 2τ, the observed echo amplitude is written by

$$V(2\tau) = \mathrm{Tr}[S_Y^A \rho(2\tau)].$$

The echo amplitude at $\tau = 0$ normalized to unity can be written as

$$V(2\tau) = \cos(D_{AB}t). \tag{1}$$

Next, we consider a special spin system composed of three different spins, A, B and C (Fig. 3). We define that θ_1 is the angle between the external magnetic field and the radius vector $\mathbf{r}_{CA}$. The angle between the external magnetic field and the radius vector $\mathbf{r}_{AB}$, θ_3 is described as

$$\cos\theta_3 = (\cos\theta_A \cos\theta_1 - \sin\theta_A \sin\theta_1)\cos\varphi,$$

$\theta_{A,B,C}$ are the angles between the vectors $\mathbf{r}_{AB}$ and $\mathbf{r}_{CA}$, $\mathbf{r}_{AB}$ and $\mathbf{r}_{BC}$, and $\mathbf{r}_{CA}$ and $\mathbf{r}_{BC}$, respectively, ($\theta_A + \theta_B + \theta_C = 180°$), and φ is the rotation angle of the triangle plane around $\mathbf{r}_{AC}$. Not only D_{CA} but also other dipole interactions D_{AB} and D_{BC} can be calculated as a function of θ_1 and φ, as the triangle is fixed in space. In this case, the spin Hamiltonian is written as

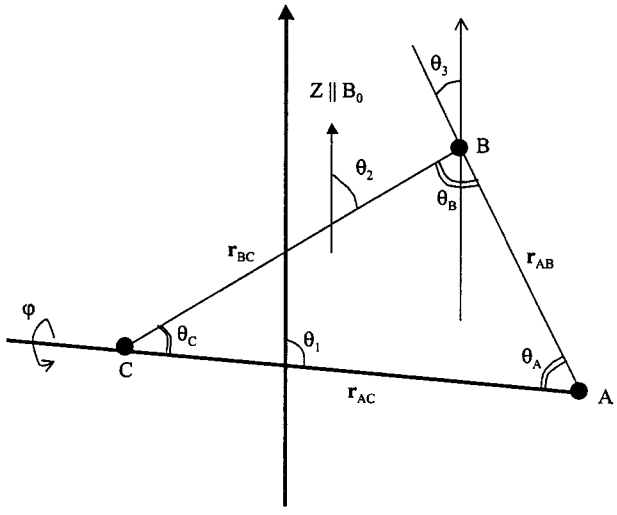

Fig. 3. Triangular configuration of three spins in which three radicals A, B and C are generated. In nonoriented system, this system is averaged over the angles θ_1 and φ.

$$\mathcal{H}/\hbar = \omega_A S_Z^A + \omega_B S_Z^B + \omega_C S_Z^C + D_{AB} S_Z^A S_Z^B + D_{BC} S_Z^B S_Z^C + D_{CA} S_Z^C S_Z^A.$$

In a frame rotating with angular frequency ω_1 resonant with the spin A, the terms that affect the A spins in the spin Hamiltonian are given by

$$\mathcal{H}/\hbar = (\Delta\omega_A + D_{AB} M_S^B + D_{AC} M_S^C) S_Z^A.$$

After calculating by density matrix, the observed echo oscillation is written as

$$V(2\tau) = \cos[(D_{AB} + D_{AC})t], \tag{2}$$

where D_{AB} and D_{AC} are the z-components of the dipolar interactions between each radical pair. In a nonoriented system, Eq. (1) or (2) is to be averaged over the angles θ and φ as shown by

$$\langle V(2\tau) \rangle \propto \int_0^{\pi} V(2\tau) \sin\theta \, d\theta d\varphi \, . \tag{3}$$

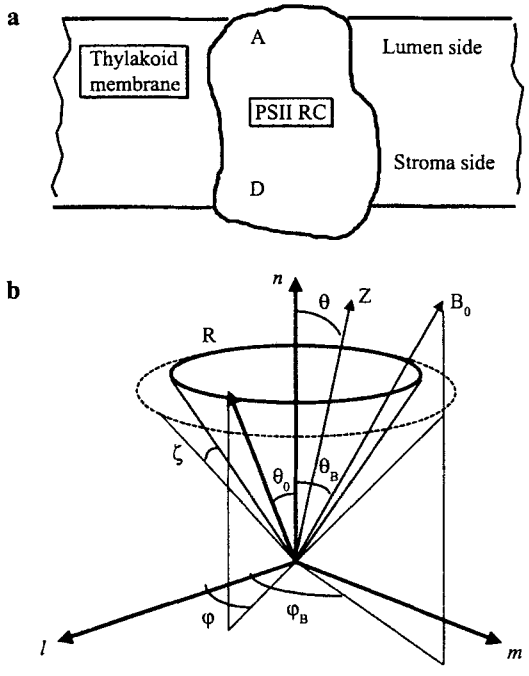

Fig. 4. Oriented PS II particle (**a**) and the definition of the axes for the membrane coordinate system (l, n, m) (**b**). The Z-axis of particles deviates from the membrane normal by a Gaussian distribution with a mean square deviation $\langle \theta^2 \rangle = \langle 15^{\circ 2} \rangle$. The deviation θ is converted to the deviation of the magnetic field direction $\zeta = B - B_0$ in simulations.

From the dipole interaction D_{ij} derived by Eq. (3), the distance between the spins A, B and C can be calculated by the point-dipole approximation.

For oriented membranes, Eq. (3) is multiplied by a Gaussian distribution function of the deviation angles from the membrane normal as given by

$$G(\theta) = \exp(-\theta^2/2\langle\theta^2\rangle),$$

where $\langle\theta^2\rangle$ is the mean square deviation which is about $\langle 15^{\circ 2}\rangle$ in our experiment (Fig. 4).

In the three-spin system, two of the three distances have already been known, the unknown distance can be derived by simulation for an assumed distance, e.g., r_{AC}. The three angles, θ_A, θ_B and θ_C, are automatically fixed.

4 Results and Discussion

The three radicals, $Y_D^{\bullet}$, $Y_Z^{\bullet}$ and Q_A^{-} were stabilized by illuminating the Zn-substituted PS II at 253 K for 20 s and then freezing at 77 K, as the Y_D radical is already present in PS II. The formation the radicals was examined by continuous-wave (CW) EPR as shown in Fig. 5. However, it is usually difficult to trap these three radicals simultaneously and the radical pairs $Y_D^{\bullet}$-$Y_Z^{\bullet}$ and $Y_D^{\bullet}$-Q_A^{-} are also present because of incomplete Zn^{2+} substitution and illumination efficiency, respectively.

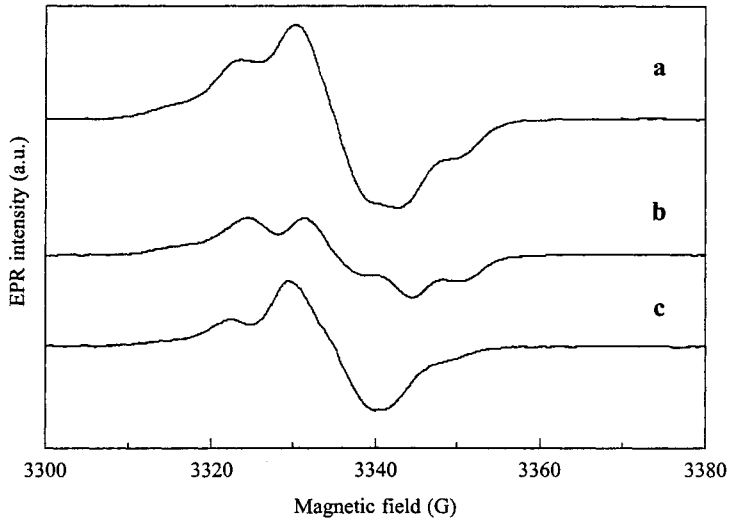

Fig. 5. **a** CW EPR spectra of trapped radicals. $Y_Z^{\bullet}$ and Q_A^{-} radical pairs were trapped by illumination at 253 K for 20 min and immediate freezing below 200 K. The spectra consist of the $Y_Z^{\bullet}$-Q_A^{-} radical pair and the stable $Y_D^{\bullet}$ radical. **b** Spectrum of $Y_D^{\bullet}$ after dark adaptation at 0°C. **c** The subtraction of spectrum **b** from spectra **a** shows the spectrum of the $Y_Z^{\bullet}$-Q_A^{-} radical pair.

The PELDOR experiment was performed at a fixed value of $\tau = 1200$ ns, with τ varying from 80 to 1200 ns. The magnetic field was fixed at the position resonating with $\omega_1 = 9.685$ GHz shown by an arrow in Fig. 6. Since the linewidth in the EPR spectrum of Q_A^- is somewhat smaller than those of the other radicals, the signals of $Y_D^\bullet$ and $Y_Z^\bullet$ (A and B) were detected with the first and third mw pulse, while the signals of Q_A^- and $Y_D^\bullet$ (C and B) or Q_A^- and $Y_Z^\bullet$ (C and A) were excited with the second mw pulse with $\omega_2 = 9.645$ GHz. Furthermore, the PELDOR time profiles of the radical pairs $Y_Z^\bullet$-$Y_D^\bullet$ and $Y_D^\bullet$-$Q_A^\bullet$ overlap on the two PELDOR signals of $Y_Z^\bullet$ (detecting $D_{ZD} + D_{ZQA}$) and $Y_D^\bullet$ (detecting $D_{DZ} + D_{DQA}$) of the three-spin system. Actually, all four time profiles are overlapped, and the observed time profile manifests summation over four time profiles with suitable ratios of each combination of the three spins. The ratios used for fitting are not the same as those in the trapped ones because the T_2 value of $Y_Z^\bullet$ is shorter than that of $Y_D^\bullet$, resulting in less contribution to the PELDOR time profile. Figure 7 shows the dependence of the primary ESE amplitude on t, measured in Zn-substituted PS II with trapped Q_A^--$Y_Z^\bullet$ pairs and $Y_D^\bullet$ radicals. In our previous work, the distance between Y_D and Y_Z was determined to be 2.96 ± 0.03 nm [12] and the distance between Y_D and Q_A was determined to be 3.85 ± 0.1 nm [17]. With these values, we made simulations of the observed time profile to find the best fitted distance between Y_Z and Q_A. In a three-spin system, the angles of the triangle encompassed by three radicals were fixed and should be taken into consideration as shown by Eq. (2). The solid curve in Fig. 7 shows the values obtained by simulation. In the simulation, we estimated the ratio of each trapped radical systems: $Y_D^\bullet$-Q_A^-, 50%; $Y_D^\bullet$-$Y_Z^\bullet$, 17%; and $Y_D^\bullet$-$Y_Z^\bullet$-Q_A^-, 33%, from the peak height of the echo signals at the corresponding time positions t in Eqs. (1) and (2). The time profile of about 67% of these signals

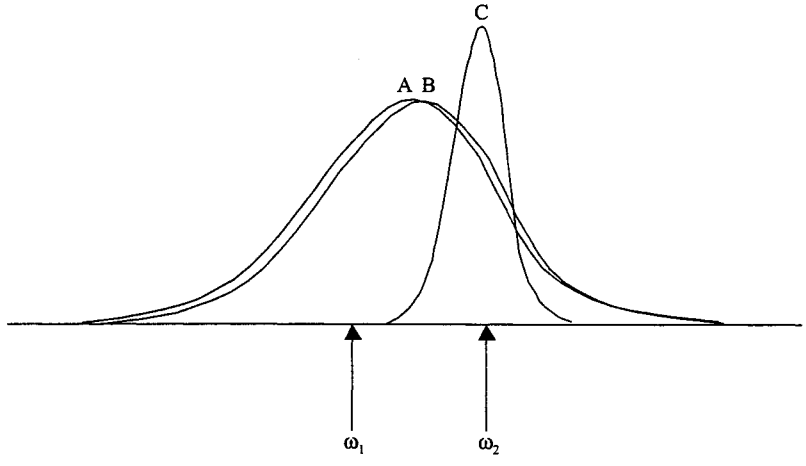

Fig. 6. Field-swept ESE spectra showing the resonance conditions of the observer ($Y_D^\bullet$ or $Y_Z^\bullet$) and the excited spins (Q_A^- and one of the other two).

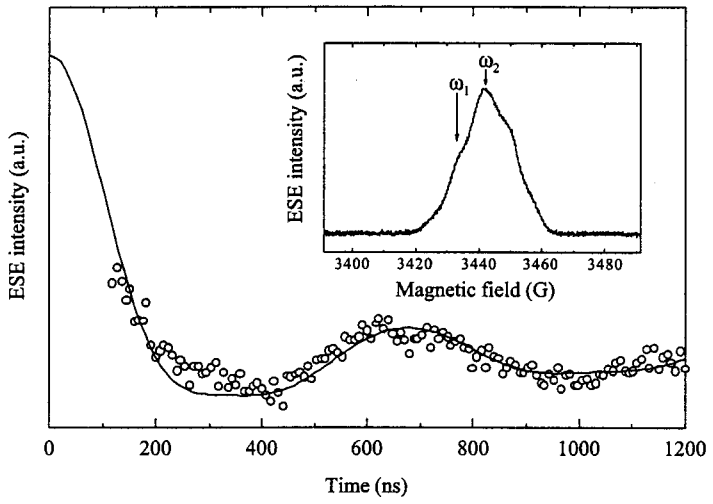

Fig. 7. PELDOR time profile of the $Y_Z^{\bullet}$-Q_A^{-}-$Y_D^{\bullet}$ three-spin system. The inset shows the field positions for detection and excitation of the PELDOR signal. Experimental data points are indicated by circles with simulated curves for the parameters of the distances $Y_D^{\bullet}$-$Y_Z^{\bullet}$ = 2.96 nm, $Y_D^{\bullet}$-Q_A = 3.85 nm and $Y_Z^{\bullet}$-Q_A = 3.4 nm and the ratios of radical systems, 33% for $Y_Z^{\bullet}$-Q_A-$Y_D^{\bullet}$, 50% for $Y_D^{\bullet}$-Q_A and 17% for $Y_D^{\bullet}$-$Y_Z^{\bullet}$. These ratios had about ±5% allowable range.

was calculated by Eq. (1) for two-spin systems. As a result of these simulations, the dipole interaction D_{ZQA} for $Y_Z^{\bullet}$-Q_A^{-} was found to be 1.32 MHz by Eq. (2). From the value of D_{ZQA}, the distance between Y_Z and Q_A is estimated to be 3.4 ± 0.05 nm. The round value $r \approx 3.4$ nm can be considered as a good estimate for the distance between Y_Z and Q_A. On the other hand, to confirm the derived distance for the three-spin system, we have obtained the distance of 3.4 ± 0.1 nm for $Y_Z^{\bullet}$-Q_A^{-} in the Y_D-less mutant of *Chlamydomonas reinhardtii* [21]. This value was the same as that obtained by Zech et al. [22] from the spin-polarized radical pair ESEEM experiment for spinach. Therefore, in this three-spin system, we could easily estimate the distance between Y_Z and Q_A.

The previous data on the oriented membranes show that the vector Y_D-Y_Z is oriented ±10° from the membrane plane. The X-ray data [5] show that Y_Z is located deeper inside the membrane. The vector from Y_D to Y_Z could be fixed at 80° from the membrane normal. The vector Y_D-Q_A is oriented 28° according to ref. 23. Then the vector Y_Z to Q_A was estimated to be oriented about 32° with the approximate value of 24° between the triangle plane and the membrane normal. Figure 8 shows the triangle fixed at the membrane coordinate system. The positions relative to Y_D (0, 0, 0) can be given by (2.92, 0, 0.51) for Y_Z and (1.73, 0.53, 3.4) for Q_A in units of nanometer.

Another three-spin system, $Y_D^{\bullet}$-Q_A^{-}-Chl_Z, was prepared by illuminating Tris-treated and Zn-substituted PS II samples at 200 K for 10 min. Figure 9 shows the time profile of the three-spin system of $Y_D^{\bullet}$-Q_A^{-}-Chl_Z^{+}. The data obtained with the "2 + 1" experiment in the oriented membranes have shown that the distance

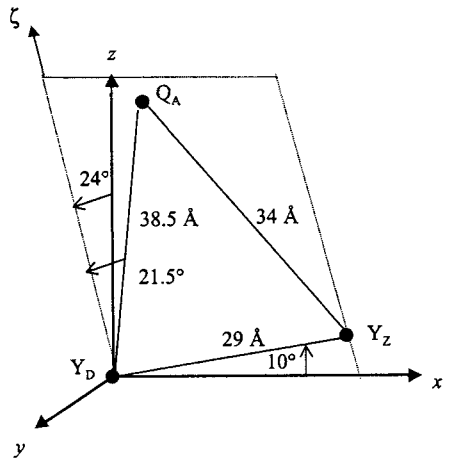

Fig. 8. Configuration of the Y_Z^+-O_A^--$Y_D^\cdot$ three spins on the basis of PELDOR. The vector Y_D-Y_Z was taken in the *zx*-plane. The plane encompassed by the triangle is inclined about 24° from the membrane normal.

between Y_D and Chl_Z and its orientation relative to the membrane normal are 2.94 nm and 50°, respectively. The distance between Y_D and Q_A and its orientation were found to be 3.85 nm [18] and 30° [24], respectively. Combining the data for Y_D-Q_A, the best-fit value of Q_A-Chl_Z was found to be 3.4 nm. In the

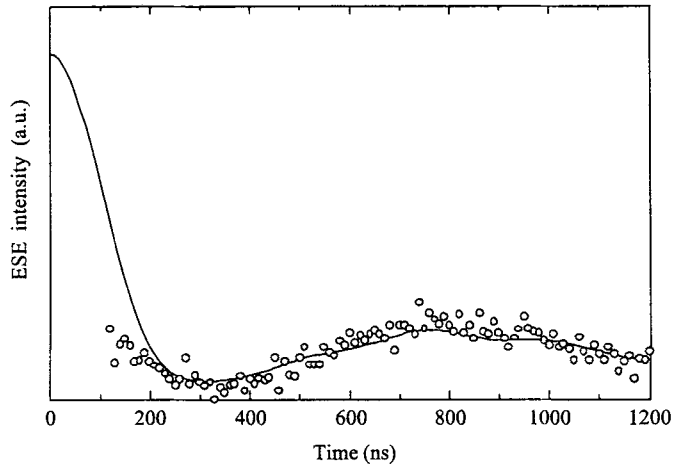

Fig. 9. PELDOR time profile of Chl_Z^+-Q_A^--$Y_D^\cdot$ observed with frequency of ω_1 = 9.650 GHz and excited with frequency ω_2 = 9.610 GHz. Circles show experimental data points and solid curve shows the best-fit simulations with the parameters for 3.4 nm for Q_A-Chl_Z, with fixed values of 2.94 nm for Chl_Z-Y_D and the same as above for Y_D-Q_A. The ratios of the radical systems were 82% for Chl_Z^+-Q_A^--$Y_D^\cdot$, 9% for Q_A-Chl_Z, and 9% for Y_D-Q_A.

Table 1. Derived distances and angles of the electron transfer cofactor molecules in PS II studied by EPR.[a]

Paramagnetic pair	Distance (nm)	Angle (°) from n axis	Method
P680-Q_A	2.74±0.03 [16]	21±5 [25]	Spin polarized ESEEM
Y_D-Q_A	3.85±0.08 [18]	32±5 [23][b]	"2 + 1" pulse
Y_Z-Q_A	3.4±0.1 [21]		PELDOR
Y_D-Y_Z	2.95±0.05 [14]	80±2 [15]	"2 + 1" pulse
Y_D-Chl_Z	2.94±0.05 [18]	50±5 [24]	"2 + 1" pulse
Y_D-$Mn_4(S_2)$	2.71±0.02 [12]	70±2 [15]	PELDOR
Q_A-Cyt *b*-559	4.0±0.3 [26]	78±5 [26]	PELDOR
Y_D-nonheme Fe	4.2±0.2 [11]		Selective hole burning
Q_A-Chl_Z	3.4±0.1[c]		3-spin PELDOR
P680-$Mn_4(S_2)$	1.5±0.5 [9]		Time resolved saturation

[a] In brackets, references are cited.
[b] The orientation was reestimated in this work.
[c] This work.

simulation, we estimated the ratio of each of the trapped radical systems: Y_D-Q_A, 9%; Q_A-Chl_Z, 9%; and $Y_D^{\cdot}$-Q_A^{-}-Chl_Z^{+}, 82%, from the peak height of the echo signals at the corresponding time positions t in Eqs. (1) and (2). The plane of this triangle is almost perpendicular to that for $Y_D^{\cdot}$-$Y_Z^{\cdot}$-Q_A^{-} in the membrane system. The derived configuration includes much more errors in the positions of each radical compared to the distances between radical pairs because the errors in orientation of the distance vectors used for derivation were about ±5°.

However, this information would help to determine the positions of small molecules of which the molecular sizes are less than the resolution of the X-ray analysis. In fact, the distance and the position of functional Chl_Z have not yet been clarified by other means. X-ray analysis could not determine the functional site and assigned two Chl_Z molecules only tentatively.

Table 1 summarizes the distances obtained so far with EPR methods. The orientations of the distance vectors were determined from the experimental data of oriented membrane samples. From Table 1 we derived the coordinates of the electron transfer components relative to Y_D at the origin (0, 0, 0). As we cannot determine absolute positions along the membrane, the directions of Y_D to Y_Z were chosen as the x-axes. The coordinates of the triangular spin configurations de-

Table 2. Coordinates of the electron transfer molecules derived from EPR data.

Cofactor molecules	x (nm)	y (nm)	z (nm)
Y_D	0	0	0
Y_Z	2.91	0	0.512
Q_A	1.86	−0.839	3.264
Chl_Z	0.836	2.1	1.896

rived in this work are shown in Table 2. The details of the derivation of Table 2 and a comparison with the X-ray data will be published elsewhere.

Acknowledgement

This work is supported by JSPS Grant-in-Aid for Scientific Research (nr. 13640412).

References

1. Miller A.-F., Brudvig G.W.: Biochim. Biophys. Acta **1056**, 1–18 (1991)
2. Rutherford A.W.: Trends Biochem. Sci. **14**, 227–232 (1989)
3. Conjeaud H., Mathis P.: Biochim. Biophys. Acta **590**, 353–359 (1980)
4. Kok B., Forbush B., McGloin M.: Photochem. Photobiol. **11**, 457–475 (1970)
5. Zouni A., Witt H.-T., Kern J., Fromme P., Kraub N., Saenger W., Orth P.: Nature **409**, 739–743 (2001)
6. Evelo R.G., Styring S., Rutherford A.W., Hoff A.J.: Biochim. Biophys. Acta **973**, 428–442 (1989)
7. Innes J.B., Brudvig G.W.: Biochemistry **28**, 1116–1125 (1989)
8. Isogai Y., Itoh S., Nishimura M.: Biochim. Biophys. Acta **1017**, 204–208 (1990)
9. Kodera Y., Takura K., Kawamori A.: Biochim. Biophys. Acta **1101**, 23–32 (1992)
10. Hirsh D.J., Beck W.F., Innes J.B., Brudvig G.W.: Biochemistry **31**, 532–541 (1992)
11. Hara H., Kawamori A.: Appl. Magn. Reson. **13**, 241–257 (1997)
12. Hara H., Kawamori A., Astashkin A.V., Ono T.: Biochim. Biophys. Acta **1276**, 140–146 (1996)
13. Milov A.D., Ponomarev A.B., Tsvetkov Yu.D.: Chem. Phys. Lett. **110**, 67–63 (1984)
14. Astashkin A.V., Kodera Y., Kawamori A.: Biochim. Biophys. Acta **1187**, 89–93 (1994)
15. Astashkin A.V., Hara H., Kawamori A.: J. Chem. Phys. **108**, 3805–3812 (1998)
16. Hara H., Dzuba S.A., Kawamori A., Akabori K., Tomo T., Satoh K., Iwaki M., Itoh S.: Biochim. Biophys. Acta **1322**, 77–85 (1997)
17. Zech S.G., Kurreck J., Eckert H.-J., Renger G., Bittl W., Bittl R.: FEBS Lett. **414**, 454–256 (1997)
18. Shigemori K., Hara H., Kawamori A.: Biochim. Biophys. Acta **1363**, 187–198 (1998)
19. Kuwabara T., Murata N.: Plant Cell Physiol. **23**, 533–539 (1982)
20. Jegerschoeld C., MacMillan F., Lubitz W., Rutherford A.W.: Biochemistry **38**, 12439–12445 (1999)
21. Kawamori A., Katsuta N., Mino H., Ishii A., Minagawa J., Ono T.: J. Biol. Phys. **28**, 413–426 (2002)
22. Zech S.G., Kurreck J., Renger G., Lubitz W., Bittl R.: FEBS Lett. **442**, 79–82 (1999)
23. Yoshii T., Kawamori A., Tonaka M., Akabori K.: Biochim. Biophys. Acta **1413**, 43–49 (1999)
24. Tonaka M., Kawamori A., Hara H., Astashkin A.V.: Appl. Magn. Reson. **19**, 141–150 (2000)
25. Yoshii T., Hara H., Kawamori A., Akabori K., Iwaki M., Itoh S.: Appl. Magn. Reson. **16**, 565–580 (1999)
26. Kuroiwa S., Tonaka M., Kawamori A., Akabori K.: Biochim. Biophys. Acta **1460**, 330–337 (2000)

Author's address: Asako Kawamori, School of Science and Technology, Kwansei Gakuin University, Sanda 665-1337, Japan